RSC Advances

ROYAL SOCIETY OF CHEMISTRY

www.rsc.org/advances

Molecularly Imprinted Polymer-Based Sensors for Atrazine Detection by Electropolymerization of o-Phenylenediamine

Xiao Li, Yanfen He, Fan Zhao, Weiying Zhang[*], Zhuoliang Ye

School of Chemical Engineering, Fuzhou University, Fuzhou 350108, China

Correspondence to: Weiying Zhang (E-mail: wyzhang@fzu.edu.cn)

Abstract

A sensitive and selective atrazine (ATZ) electrochemical sensor was developed based on molecularly imprinted polymer (MIP). The density functional theory at B3LYP/6-31G (d, p) level and Gaussian 2009 package was used to calculate the interaction energy of template-monomers. The MIP sensing film was prepared by electropolymerization of o-phenylenediamine (o-PD) using ATZ as the template. Some factors affecting the activity of the sensor have been discussed. The performance of the sensor was characterized by cyclic voltammetry and differential pulse voltammetry. Under the optimal experimental conditions, the relative current change was linear to the concentration of ATZ in the range of 5.0×10^{-9} to 1.4×10^{-7} M with a detection limit of 1.0×10^{-9} M. The result of selectivity experiment showed that imprint electrode has good response and selectivity towards ATZ. The proposed MIP-based sensor also showed a good stability and repeatability.

Keywords: Atrazine; Density functional theory; Electrochemical sensor; Electropolymerization; Molecularly imprinted polymer

1. Introduction

Atrazine (ATZ) is conventional triazine herbicide which has widely been used in the annual control of some grasses and broadleaf weeds in corn, sugar cane, sorghum, and other cultures.[1,2] ATZ has strong lethality on weed and its price is cheap. But after a

long period of study, it has been found that ATZ is harmful for people and animals. Therefore, ATZ is classified as a priority pollutant which is currently prohibited according to the EC legislation (Commission Decision 2004/248/EC). ATZ has good water solubility, long residual period, and can exist in environment for a long time.[3-5] Thus, the detection of ATZ has become more and more important.

Techniques to determine trace amount of ATZ in the environment include spectrophotometric,[6,7] high performance liquid chromatography (HPLC)[8-10] and gas chromatography (GC).[11,12] However, these techniques require complicated sample preparation usually involving pre-concentration, which is expensive and time-consuming. Thus, a simple, highly sensitive and selective method for trace ATZ detection is highly desirable in routine analytical practice.

Electrochemical sensors have the advantages of high sensitivity, simple operation and low cost. It has been used in detection of environmental pollutants.[13] The core of electrochemical sensors is recognition elements which can identify and combine with the specific target analytes. MIP is highly selective functional materials. The structure of MIP has many imprinted cavities that match with template molecule in shape and size.[14] MIP has been widely used in chromatographic separation, solid-phase extraction, enzyme-mimic catalysis and molecular recognition sensors.[15-19] Recently, Molecularly imprinted electrochemical sensors (MIECS) which use MIP as the recognition element has attracted extensive attention.[20,21] MIP has several advantages over biologically recognition element, including high affinity, high selectivity, and inexpensive.

There have been many reports about ATZ detection by MIPs based electrochemical sensors.[22-24] Pardieu et al.[25] have developed an electrochemical sensor based on molecularly imprinted conducting polymer for detection of ATZ. The MICP, poly(3,4-ethylenedioxythiophene-co-thiophene-acetic acid), has been electrochemically synthesized onto a platinum electrode. The developed sensor showed a good selectivity for ATZ and low detection limit (10^{-7} M). Liu et al.[26] have developed a core-shell nanostructure molecular imprinting fluorescent chemosensor for selective detection of ATZ. The sensor showed a detection limit (LOD) of about 1.8 μM and high selectivity for ATZ. o-Phenylenediamine (o-PD) is easy to be electropolymerized on various

substrates to form films with good chemical and mechanical stability.[27-29] There were many preparations of MIECS with o-PD as functional monomer was reported.[30,31] This method has the advantage of easy and fast, which don't need a crosslinking agent and solvent.

In this work, the interaction between o-PD and ATZ was calculated by using the density functional theory (DFT) method in order to optimize the ratio of ATZ to o-PD. MIP film was then prepared by electropolymerizing o-PD in the presence of ATZ, and an ATZ electrochemical sensor based on MIP sensing film was developed. The developed sensor showed specific recognition toward ATZ with a rather low detection limit of 1.0×10^{-9} M.

2. Experimental

2.1. Materials

Atrazine, simazine and alachlor were bioreagent purchased from Shandong Qiaochang Chemical Co., Ltd. (China). o-Phenylenediamine, potassium ferricyanide and potassium ferrocyanide were analytical grade obtained from Sinopharm Chemical Reagent Company (China). All other reagents were of analytical grade and were used without further purification. Phosphate buffer solution (PBS, pH 7.4) was prepared by mixing 0.1 M Na_2HPO_4 and NaH_2PO_4. All solutions were prepared with D.I. water.

2.2. Apparatus

Electrochemical measurements were performed on a CHI660 electrochemical workstation (Shanghai Chenhua Instrument Co., Ltd., China) coupled with a conventional three-electrode cell. The three-electrode system consists of a saturated calomel electrode as the reference electrode, a platinum wire electrode as the auxiliary electrode and a bare or polymer-modified gold electrode (2 mm in diameter) as the working electrode.

2.3. Computational calculation

All calculations were carried out using Gaussian 09 software package. Conformation optimization of ATZ, o-PD and their complexes was performed by DFT at B3LYP/6-31G (d, p) level. The electronic stabilization energy, ΔE, was calculated through Equation (1).

$$\Delta E = E \text{ (ATZ-o-PD complex)} - E \text{ (ATZ)} - \sum E \text{ (o-PD)} \qquad (1)$$

2.4. Preparation of MIP-based sensor

Molecular self-assembly was achieved by mixing 1 mM ATZ and 5 mM o-PD in PBS (pH=7.4) for 5 h. Gold electrode surface was polished to a mirror finish using aqueous slurry of 0.05 μm alumina particles before washed with water and ethanol in an ultrasonic cleaner. Then the electrode was subjected to cyclic potential sweeps between -0.1~1.4 V in 0.5 M H_2SO_4 until stable cyclic voltammograms was obtained. Next, MIP was prepared on the gold electrode by electropolymerization in the self-assembled solution. Fifteen cycles of cyclic voltammograms were performed in the potential range of 0-0.8 V (scan rate 50 mV/s). The gold electrode with MIP film was then washed in the mixed solvent of methanol/acetic acid (9:1 v/v) to remove the templates. A MIP-based sensor with stereo cavities in imprinted membranes was obtained. The scheme of preparation was showed in Fig 1.

A gold electrode with non-imprinted film was prepared following the same procedure as above but in the absence of ATZ.

2.5. Electrochemical measurement

All the electrochemical measurements were carried out in 5 mM $K_3[Fe(CN)_6]/K_4[Fe(CN)_6]$ solution containing 0.1 M KCl at room temperature. Cyclic voltammetry (CV) measurements were performed over a potential range from -0.1 V to 0.5 V with a scan rate of 50 mV/s. Differential pulse voltammetry (DPV) measurements were conducted from -0.1 V to 0.5 V. The amplitude, width and period of pulse were 50 mV, 50 ms and 200 ms, respectively. Before electrochemical measurements, the solution

was purged with N_2 for 10 min.
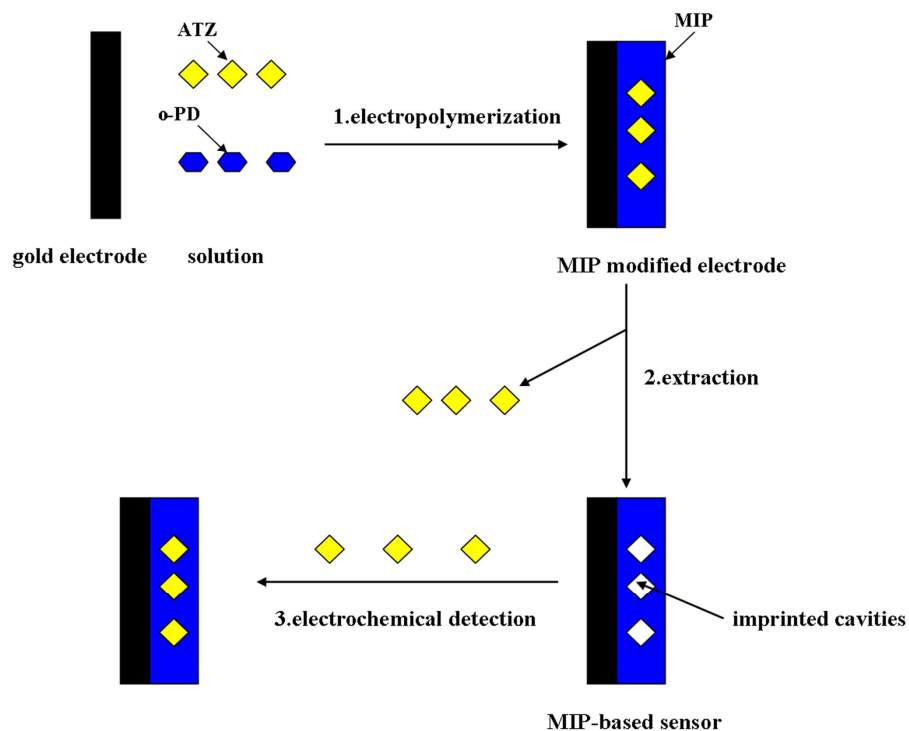
Fig 1. Schematic representation of the preparation and the use of MIP-based sensor.

2.6. Determination of ATZ

DPV measurements were performed in 5 mM $K_3[Fe(CN)_6]$/ $K_4[Fe(CN)_6]$ solution containing 0.1 M KCl after the imprinted electrode was incubated in aqueous solutions containing different concentrations of ATZ for 8 min. Relative current change ($\Delta I/I_0$) was employed to characterize the adsorption of modified electrode for ATZ. Herein, I_0 is the peak current in background solution and ΔI is the difference between I_0 and the peak current in the presence of ATZ.

2.7. Selectivity toward ATZ

The selectivity of the MIP-based sensor for ATZ was tested by DPV. The selectivity factor, α, was used to represent the selectivity and was calculated according to Equation (2).

$$\alpha = (\Delta I/I_0)_{ATZ} /(\Delta I/I_0)_{\text{interferent}} \tag{2}$$

Simazine and alachlor were chosen as the interferents. The structures of ATZ, simazine and alachlor were showed in Fig 2.
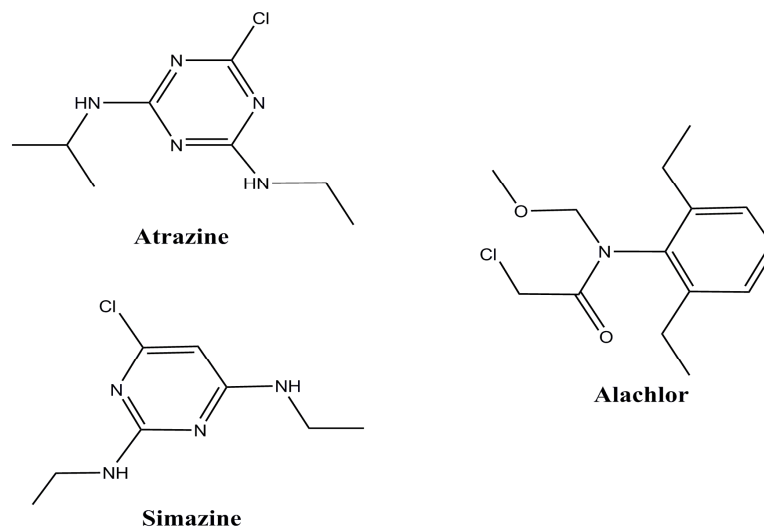
Fig 2. The structure of ATZ and interferents

3. Results and discussion

3.1. Computational simulation of ATZ and o-PD complex

The configurations of ATZ, o-PD and ATZ-o-PD complexes were constructed and optimized by DFT at B3LYP level with 6-31G (d, p). The results were shown in Fig 3. The binding energy between ATZ and o-PD with different ratios (1:1, 1:2, 1:3, 1:4) was calculated and the results were summarized in Table 1. A complex with higher absolute value of ΔE predicts a more stable configuration. As it was observed, the absolute value of ΔE increased with increasing proportion of o-PD. When the ratio of ATZ to o-PD was 1:4, the binding energy had the minimum value of -92.682kJ/mol, and the complex was the most stable. When the ratio was 1:5, stable complex configuration wasn't obtained by calculation. This might be attributed to the steric hindrance, resulting in the increasing repulsive force between ATZ and o-PD. The distance between molecules

increased and the active sites of hydrogen bond reduced. The stability of complex became weak.

Table 1 Binding energies (ΔE) of complexes calculated at B3LYP level.

Mole ratio of ATZ to o-PD	E (Hartree)	ΔE (Hartree)	ΔE (kJ/mol)
1:0	-1047.310225	-	-
0:1	-342.975005	-	-
1:1	-1390.299518	-0.01428845	-37.51432548
1:2	-1733.283434	-0.02319904	-60.90907952
1:3	-2076.265512	-0.03027203	-79.47921477
1:4	-2419.245546	-0.03530073	-92.68206662
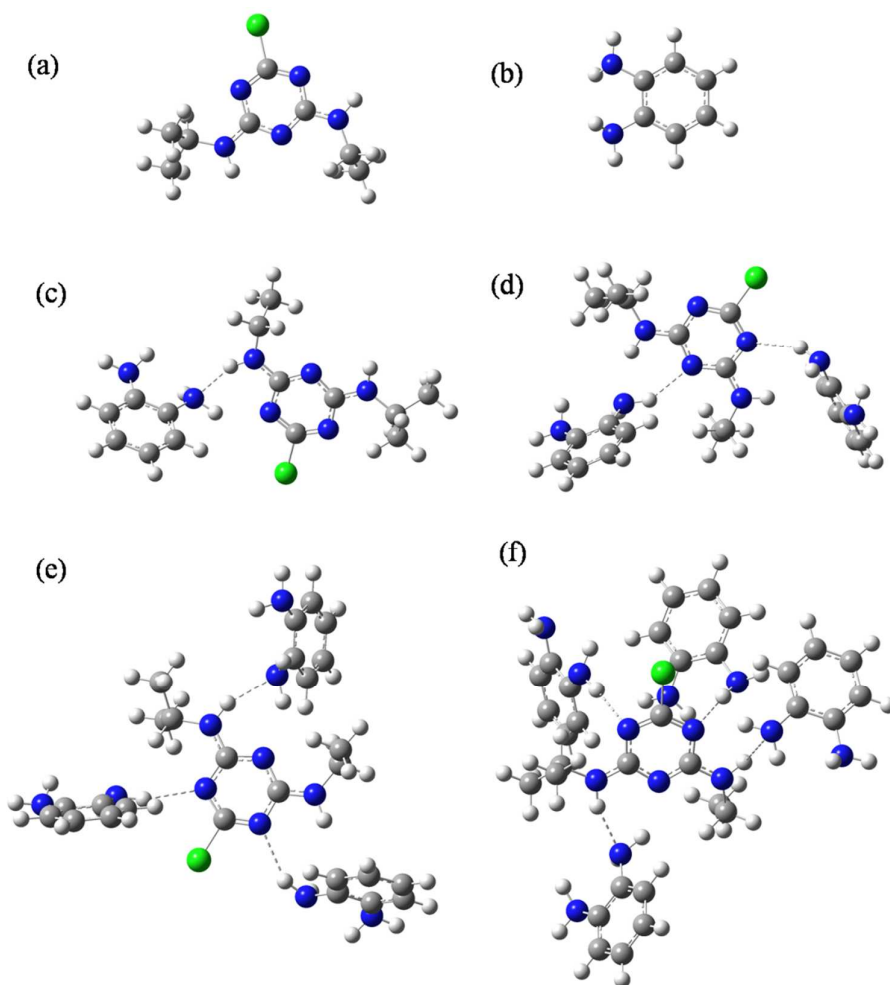
Fig 3. Optimized conformations of ATZ, o-PD and their complexes by DFT. (a) ATZ; (b) o-PD; (c) ATZ+o-PD; (d) ATZ+2o-PD; (e) ATZ+3o-PD; (f) ATZ+4o-PD.

3.2. Electropolymerization for MIP-based sensors

3.2.1. Formation of the MIP sensing film

Fig 4 shows the cyclic voltammogram recorded during the electropolymerization of o-PD in the present of ATZ on the gold electrode. In the first scan cycle, the o-PD oxidation was visible at 0.27 V and the peak current was 5.082×10^{-5} A, but the reduction peak can't be observed. The result showed that the process of electropolymerization of o-PD was completely irreversibly. Then the peak current dropped significantly with each scan cycle, finally, the current tend to zero. The result means that the electrode surface covered with a layer of dense polymer membranes, and the conductivity of membrane is low. The polymer membranes hindered o-PD monomer oxidizing reaction on the gold electrode surface.
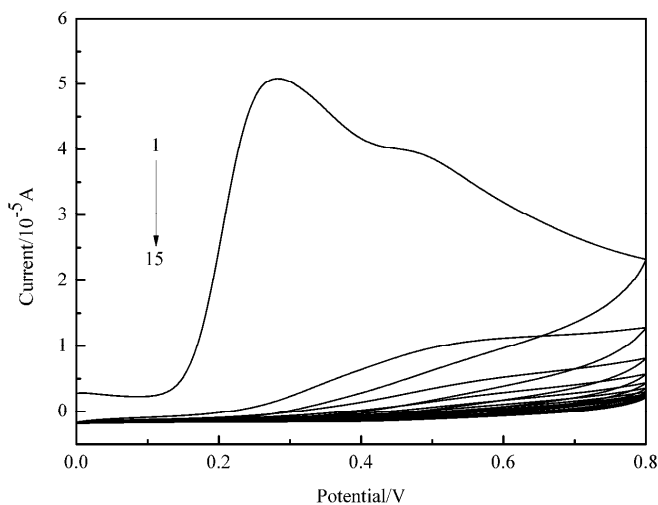
Fig 4. Electropolymerization of o-PD on a bare gold electrode by CV.
Polymerization condition: 5 mmol/L o-PD+1 mmol/L ATZ, pH=7.4, scanning rate 50mV/s.

3.2.2. Effect of the number of C scan cycle

The optimum number of CV scan cycle during electropolymerization process was

explored in order to improve the sensitivity and stability of the sensor. Five imprinted electrodes were prepared with different scan cycles (7, 10, 15, 20, 25) and used to detect 5×10^{-8} M ATZ. As shown in Fig 5(A), the relative current change reached maximum when the number of scan cycle was 15. When the number of scan cycle was more than fifteen, the imprinted polymer film was so thick that ATZ molecules situated at the central area of the polymer film could not be completely removed from polymers matrix. The imprinted polymer films became very rough when the number of scan cycle was too less, which led to enhancement of nonspecific adsorption and less recognition of ATZ. Therefore, fifteen cycles was chosen as the optimum scan cycles during the electropolymerization process.
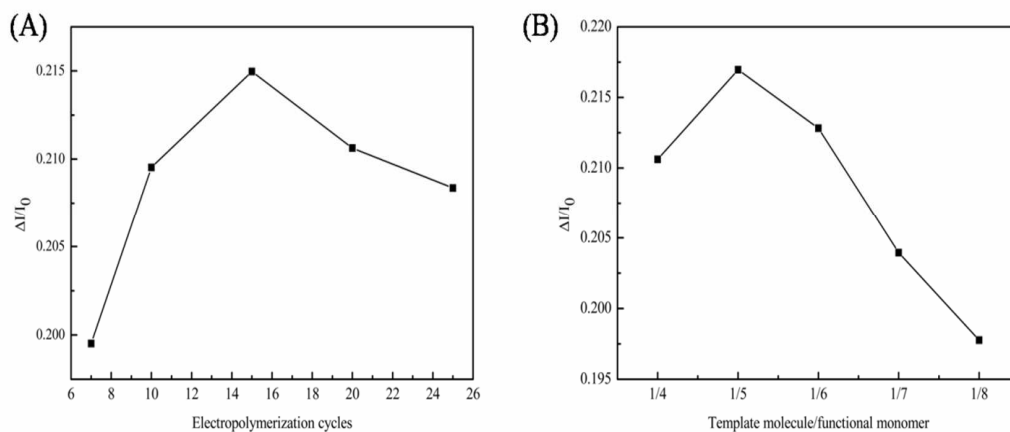
Fig 5. Effect of scan cycles (A) and mole ratios of ATZ to o-PD (B) during the electropolymerization on the relative current response of MIP-based sensor.

3.2.3. Effect of the mole ratio of ATZ to o-PD

The mole ratio of template molecule to functional monomer during the self-assembly process affects the shape and performance of imprinted membranes. Excessive use of functional monomer is usually good for forming more non-covalent binding sites in polymer film. In this work, the molar ratio of template ATZ to functional monomer o-PD was changed from 1:4 to 1:8 while the concentration of o-PD kept 5mM. Fig 5(B) showed the relative current change of imprinted electrodes with different ratios of ATZ to o-PD. The great relative current change appeared at the ratio of 1:5. When the ratio was less than 1:5, the quantity of available binding sites reduced

due to the lower concentration of ATZ. Moreover, the excessive o-PD might lead to increase of non-selective binding sites generated by surplus o-PD, and decrease of the specific adsorption to ATZ. When the ratio was more than 1:5, the amount of functional monomer was not enough to combine all the template molecules. The molar ratio of 1:5 was considered suitable for production of MIP film. It is somewhat inconsistent with the result of computational modeling. The reason was that there was electrostatic attraction between ATZ and o-PD besides hydrogen bond.

3.3.   Electrochemical characterization of MIP and NMIP electrodes

Cyclic voltammograms of different electrodes in 5 mM $K_3[Fe(CN)_6]$/ $K_4[Fe(CN)_6]$ solution containing 0.1 M KCl were shown in Fig 6(A). Curve a showed a pair of typical redox peaks of ferricyanide probe occurring on the surface of the bare gold electrode. From curve a to b, the peak current decreased to near zero, which indicated that a nonconductive polymer film was formed on the electrode surface and hindered the redox probe from getting access to the surface of the electrode. After the removal of ATZ, the peak current increased (curve c). It showed that ATZ molecules were eluted from the polymer film, leaving cavities and the probe obtained the access to the electrode surface. When the imprinted film rebound ATZ, the cavities were again blocked and the peak current decreased (curve d). But it was higher than that of curve b, because some cavities might be deformed to hinder the entrance of ATZ molecules.

As for the NMIP electrode (Fig 6(B)), the peak current decreased greatly from curve a to e, because the poly (o-PD) film in the absence of ATZ covered the surface of the gold electrode. The change of current was negligible from curve e to f, because no imprinted cavities were obtained after the NMIP electrode being washed with the mixed solvent of methanol/acetic acid.
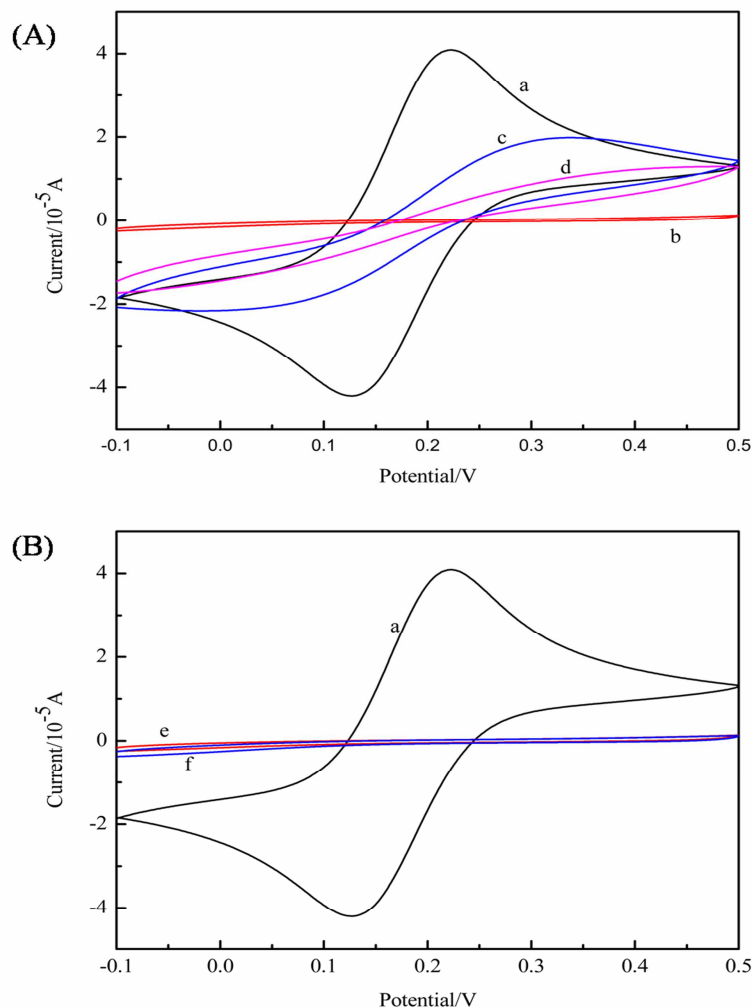
Fig 6. CVs of gold electrodes modified with different films. (a) Bare gold electrode; (b) imprinted film before removal of ATZ; (c) imprinted film after removal of ATZ; (d) imprinted film after rebinding with ATZ; (e) non-imprinted film before soaking; (f) non-imprinted film after soaking. The scan rate was 50 mV/s.

3.4. Detection range of ATZ

The DPV current responses of the imprinted electrode to the concentrations of ATZ were displayed in Fig 7. The peak current decreased with increasing ATZ concentration. The inset in Fig 7 showed the relationship between the relative change of peak current and the concentration of ATZ. The relative current change increased

linearly with the concentration of ATZ between 5.0×10^{-9} and 1.4×10^{-7} M. The linear regression curve was shown as Equation (3) with a coefficient of correlation of 0.998. And the detection limit was 1.0×10^{-9} M.

$$\Delta I/I_0 = 0.03831 \; c \; (10^{-8} \, \text{M}) + 0.02422 \qquad (3)$$
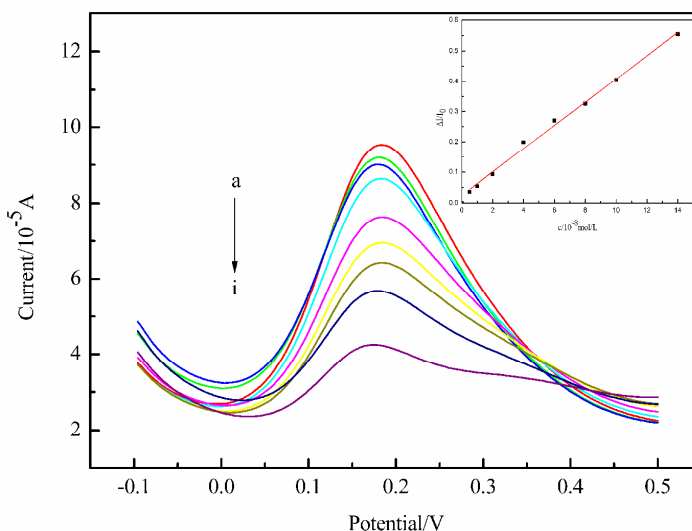
Fig 7. DPV of the imprinted electrode at different concentrations of ATZ (a→i): (0, 0.5, 1, 2, 4, 6, 8, 10 and 14) $\times 10^{-8}$ M ATZ, respectively. Amplitude: 50 mV; width: 50 ms; period of pulse: 200 ms.

3.5. Selectivity of imprinted electrode

In order to check the specificity of recognition of the MIP-based sensor towards ATZ, simazine and alachlor were chosen as the interferents. The responses to simazine and alachlor of the imprinted electrode were measured by DPV. The relative change of peak current to simazine and alachlor were showed in Fig 8(the data was shown in Table S1, supplement information). The results showed that ATZ produced higher current changes than simazine, which meant that there was a weak recognition of simazine in comparison with ATZ. The reason was that both simazine and ATZ belong to triazine family and present two side-chain amino groups. Therefore, simazine may establish hydrogen-bonds with the nitrogen and hydrogen atoms of poly(o-PD) at the surface of MIP cavities. Alachlor, however, produced almost negligible current changes due to its fundamentally different structure compared to ATZ. This pesticide did not

match the functionalized cavities of MIP film even if it could establish hydrogen-bonds. The specificity of recognition of the NIP-based sensor towards ATZ was explored as MIP-based sensor, but the result showed that the NIP-based sensor have almost no response to ATZ.
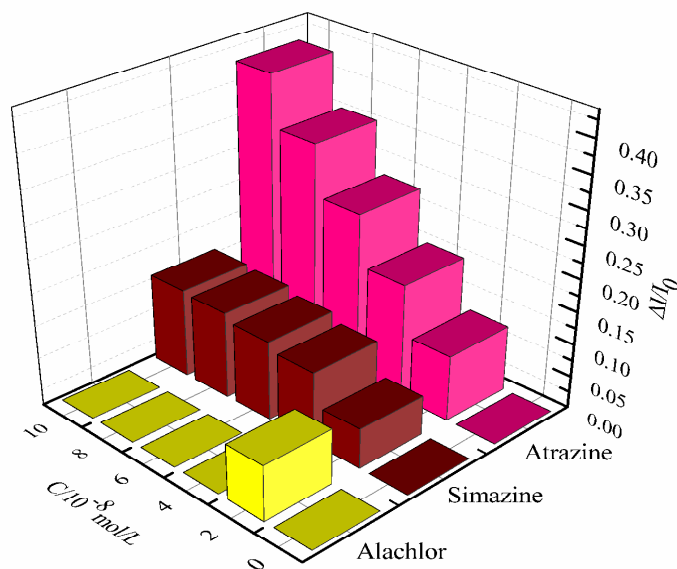
Fig 8. Relative current change of imprinted electrode to ATZ and analogues at different concentrations.

Table 2 showed that selectivity factors of MIP-sensors toward different concentrations of interferents were more than 1, so the MIP-sensors have selectivity for ATZ.

As a conclusion, the developed MIP sensor displays a selective recognition towards ATZ.

Table 2 The selectivity of MIP-modified electrode for ATZ and interferents

concentration/	α	
10^{-8} M	Simazine	Alachlor
2	1.66	1.19
4	1.60	∞
6	2.07	∞
8	2.49	∞
10	3.00	∞

3.6. Stability and repeatability

To ensure the stability, the imprinted electrode was stored at room temperature for a period of time before being used. The current response decreased about 3.6% after a week, and decreased about 13.3% after two weeks. It was demonstrated that the imprinted electrode had fairly good stability. The repeatability of the imprinted electrodes was investigated by detecting 1×10^{-8} M of ATZ. The calculated RSD in six parallel tests was about 5.43%. This result confirmed that the sensor had good test repeatability.

The recovery of imprinted electrode also was studied and the data was shown in Table 3. The results showed that the recovery of imprinted electrode ranged from 95.5% to 103.5%.

Table 3 Recovery of atrazine

Added (10^{-8} mol·L^{-1})	Found (10^{-8} mol·L^{-1})	Recovery (%)
2.00	2.07	103.5
2.00	1.91	95.5
2.00	1.94	97.0
4.00	3.86	96.5
4.00	3.89	97.3
4.00	3.93	98.3
8.00	7.92	99.0
8.00	7.88	98.5
8.00	8.12	101.5

4. Conclusions

A MIP-based electrochemical sensor for ATZ was successfully constructed by the electropolymerization of o-PD on the surface of a gold electrode in the presence of ATZ. The specific imprinted electrode showed sensitivity and selectivity toward ATZ. The MIP-based sensor exhibited a rather low detection limit down to 1×10^{-9} M in a linear

detection range from 5.0×10^{-9} to 1.4×10^{-7} M. The sensor showed good stability and repeatability.

Acknowledgments

References

1 L. Svorc, M. Rievaj and D. Bustin, *Sensor Actuat B-Chem.*, 2013, **181**, 294-300.

2 K. Prasad, K. P. Prathish, J. Mary Gladisa, G. R. K. Naidu and T. Prasada Rao, *Sensor. Actuat B-Chem.*, 2007, **123**, 65-70.

3 H. Xing, X. Wang, G. Sun, X. Gao, S. Xu and X. Wang, *Environ. Toxicol. Pharm.*, 2012, **33**, 233-244.

4 M. Kucka, K. Pogrmic-Majkic, S. Fa, S. S. Stojilkovic and R. Kovacevic, *Toxicol. Appl. Pharm.*, 2012, **265**, 19-26.

5 J. G. Gu, Y. Z. Fan and J. D. Gu, *Chemospehre.*, 2003, **52**, 1515-1521.

6 G. Zhang and J. Pan, *Spectrochimi. Acta.*, *A.* 2011, **78**, 238-242.

7 E. Ayranci and N. Hoda, *J. Hazard. Mater.*, 2004, **112**, 163-168.

8 Z. Kuklenyik, P. Panuwet, N. K. Jayatilaka, J. L. Pirkle and A. M. *Calafat, J. Chromatogr B. Analyt. Technol. Biomed. Life. Sci.*, 2012, **901**, 1-8.

9 R. X. Mou, M. X. Chen, Z. Y. Cao, Z and W. Zhu, *Anal. Chimi. Acta.*, 2011, **706**, 149-156.

10 M. T. Muldoon and L. H. Stanker, *Anal. Chem.*, 1997, **69**, 803-808.

11 B. D. Real, M. C. Ortiz and L. A. Sarabia, *J. Chromatogr. B.*, 2012, **910**, 122-137.

12 I. K. Konstantinou, T. M. Sakellarides, V. A. Sakkas and T. A. Albanis, *Environ. Sci. Technol.*, 2001, **35**, 398-405.

13 M. J. Schöning, R. Krause and K. Block, *Sensor. Actuat B-Chem.*, 2003, **95**, 291-296.

14 P. A. Cormack and A. Z. Elorza, *J. Chromatogr. B.*, 2004, **804**, 173-182.

15 F. Lanza and B. Sellergren, *Chromatogr.*, 2001, **53**, 599-611.

16 X. F. Zheng, Q. Lian and H. Yang, *RSC Adv.*, 2014, **4**, 42478-42485.

17 Q. Fu, H. Sanbe, C. Kagawa, K. K. Kunimoto and J. Hagina, *Anal. Chem.*, 2003, **75**, 191–198.

18 G. Wulff, *Chem Rev.*, 2002, **102**, 1-27.

19 C. M. Dai, X. F. Zhou and Y. L. Zhang, *J. Hazard. Mater.*, 2011, **198**, 175-181.

20 T. Alizadeh and S. Amjadi, *J. Hazard. Mater.*, 2011, **190**, 451-459.

21 W. R. Huang, Y. L. Chen, C. Y. Lee and H. T. Chiu, *RSC Adv.*, 2014, **4**, 62393-62398.

22 R. Shoji, T. Takeuchi and I. Kubo, *Anal. Chem.*, 2003, **75**, 4882-4886.

23 T. A. Sergeyeva, O. V. Piletska, S. A. Piletsky, L. M. Sergeeva, O. O. Brovko and G. V. El'ska, *Mater. Sci. Eng. C.*, 2008, **28**, 1472-1479.

24 D. Lakshmi, M. Akbulut, P. K. Ivanova-Mitseva, M. J. Whitcombe, E. V. Piletska, K. Karim, O. Guven and S. A. Piletsky, *Ind. Eng. Chem. Res.*, 2013, **52**, 13910-13916.

25 E. Pardieu, H. Cheap, C. Vedrine, M. Lazerges, Y. Lattach, F. Garnier, S. Remita and C. Pernelle, *Analytica. Chimica Acta.*, 2009, **649**, 236-245.

26 R. Liu, G. Guan, S. Wang and Z. Zhang, *Analyst.*, 2011, **136**, 184.

27 Z. L. Cheng, E. K. Wang and X. R. Yang, *Biosens. Bioelectron.*, 2011, **6**, 179-185.

28 J. P. Li, S. H. Li, X. P. Wei, H. L. Tao and H. C. Pan, *Anal. Chem.*, 2012, **84**, 9951-9955.

29 Y. Liu, Q. J. Song and L. Wang, *Microchem. J.*, 2009, **91**, 222-226.

30 X. Wen, X. Li, W. Y. Zhang and X. G. Ying, *Chem. J. Chinese. U*, 2012, **33**, 2199-2204.

31 Z. Cheng, E. Wang and X. Yang, *Biosens. Bioelectron.*, 2001, **16**, 179-185.

Supplement Information

Table S1 The relative change of peak current of MIP-modified electrode for ATZ and interferents

concentration/ 10^{-8} M	$\Delta I/I_0$		
	Atrazine	Simazine	Alachlor
2	0.10084	0.06081	0.08447
4	0.17746	0.11082	0
6	0.25408	0.12265	0
8	0.33070	0.13256	0
10	0.40732	0.13582	0